Photoionization of ozone: Formation of O4 + and O5 +

Morris J. Weiss, J. Berkowitz, and E. H. Appelman

Citation: The Journal of Chemical Physics **66**, 2049 (1977); doi: 10.1063/1.434164
View online: http://dx.doi.org/10.1063/1.434164
View Table of Contents: http://scitation.aip.org/content/aip/journal/jcp/66/5?ver=pdfcov
Published by the AIP Publishing

Photoionization of ozone: Formation of O_4^+ and O_5^+*

Morris J. Weiss,† J. Berkowitz, and E. H. Appelman

Argonne National Laboratory, Physics Division, Argonne, Illinois 60439
(Received 25 October 1976)

Ionization yields of O^+, O_2^+, and O_3^+ have been studied as a function of wavelength in the photoionization of ozone from threshold to 600 Å with the primary process being the production of O_3^+. The ratio $O_3^+:O_2^+:O^+$ at 600 Å is 1.00:0.36:0.05. The adiabatic ionization potential of O_3^+ is 990.32±0.3 Å (12.519±0.004 eV). Steplike structure occurs near threshold, at wavelengths corresponding to vertical ionization potentials reported in photoelectron spectroscopy studies. A weak onset for O_2^+ production appears at 13.08_2 eV (947.7 Å), followed by more intense O_2^+ production at 13.43_2 eV (932.2 Å). The onset for O^+ formation appears weakly at 15.21 eV, rising continuously with decreasing wavelength. The formation of O_5^+ via the ion–molecule reaction $O_3^+ + O_3 \rightarrow O_5^+ + O$ was also observed and measured as a function of wavelength. The O_4^+ ion was also detected. Pressure dependences and enthalpy considerations make the reaction $O_3^+ + O_2 \rightarrow O_4^+ + O$ a highly probable mechanism for O_4^+ formation.

I. INTRODUCTION

Recently there has been renewed interest in ozone and its behavior toward various atmospheric pollutants.

There have been many studies of photoabsorption of ozone in the ultraviolet.[1] In the vacuum ultraviolet, Tanaka, Inn, and Watanabe[2] reported measurements between 1050 and 2200 Å. Ogawa and Cook[3] later extended the region down to 520 Å.

The first reported photoionization mass spectrometric study of ozone using dispersed light was that of Cook[4] in 1970 using low resoultion and relatively higher sample pressures than those used in the present study. We report here photoionization efficiency curves for the O_2^+ and O^+ fragments from O_3 as well as O_3^+ and O_5^+ produced in an ion–molecule reaction between O_3^+ and O_3.

II. APPARATUS

The one-meter McPherson near-normal incidence monochrometer and the single focusing 60° 12 in. radius of curvature magnetic mass spectrometer used in this study have already been described in previous publications[5] and will not be discussed here. The Hopfield continuum was used with 50 μ entrance and exit slits. Because of the need for better light intensity near threshold, the hydrogen many-lined spectrum was also used in the region 1000–955 Å.

The monochromator employed two gratings. A 600 lines/mm gold-coated grating blazed for 800 Å and a 1200 lines/mm MgF_2 coated grating blazed for 1200 Å were used with both the Hopfield continuum and hydrogen many-lined spectrum.

The automatic data acquisition system was similar to that described earlier and will not be elaborated upon here. Ion signals were generally accumulated over periods of 40 sec, with wavelengths scanning over intervals of 0.25 Å and 0.125 Å.

III. EXPERIMENTAL PROCEDURE

Ozone was introduced into a sample inlet system modified for handling corrosive gases. All copper was replaced by stainless steel. The ozone was stored in a silica gel trap immersed in an acetone–dry ice bath. The sample pressure was regulated by a teflon needle valve connected to the silica gel trap. Ozone was introduced into the ionization chamber region to an optimum chamber pressure of 2×10^{-5} Torr for the O_5^+ studies. Under these conditions the pressure in the ionization chamber itself was estimated to be 2×10^{-4} Torr.

IV. EXPERIMENTAL RESULTS AND DISCUSSION

A. O_3^+

The photoionization efficiency curve for O_3^+ is shown in Fig. 1 and in greater detail over a limited wavelength range in Fig. 2. The general features can be described as a weak adiabatic onset at 12.519±0.004 eV, followed by a series of rounded steps separated on the average by an interval of 655±60 cm^{-1}. The O_3^+ photoionization efficiency curve levels off at about 950 Å. The curve then rises continuously to a maximum in the region 785–790 Å. Two additional maxima appear at 735 Å and 695 Å. The O_3^+ intensity then falls off to 600 Å, the usable limit of the Hopfield continuum.

The Hopfield continuum is relatively inefficient in the region of the onset for O_3^+. Furthermore because of a grating peculiarity, an experimental artifact appeared and was coincident with several intense OI emission lines that were always present with the continuum. The artifacts show up as bimodal peaks and are seen in Fig. 1, in the 971–950 Å region.

To confirm that all the steplike structure observed was real, the threshold region was studied with the hydrogen many-lined spectrum, which, although not a continuum, is nevertheless relatively efficient in the region where the adiabatic onset for O_3^+ is expected to be weak. In addition, the grating was exchanged for a 1200 lines/mm magnesium fluoride coated grating blazed for 1200 Å. The photoionization efficiency curve for O_3^+ taken under these conditions is shown in Fig. 3, where the photoionization measurements again confirm the existence of six or seven steplike onsets. The appearance of an additional step in both photoionization efficiency curves taken under different grating and source conditions may reflect the presence of an additional vi-

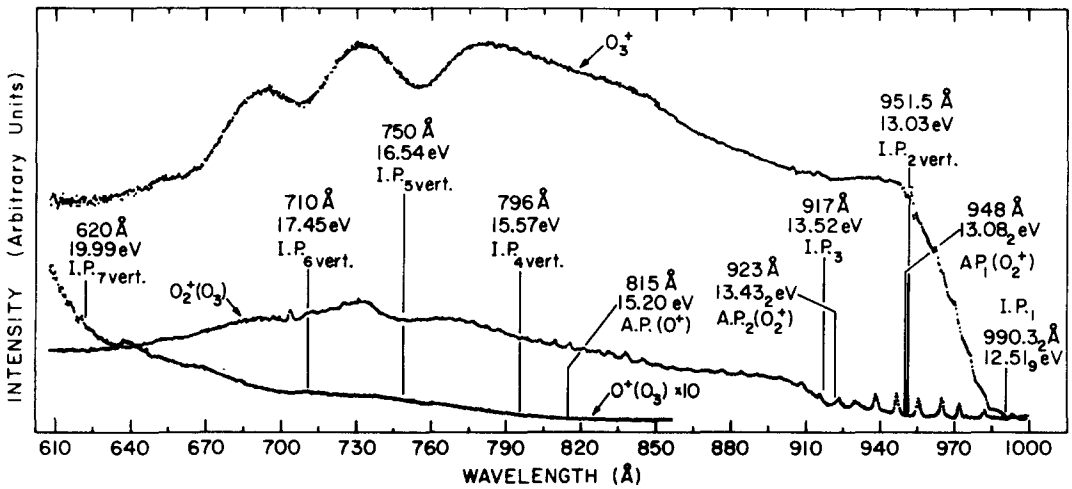

FIG. 1. Photoionization efficiency curves for O_3^+, O_2^+, and O^+ from ozone. The structure superimposed on the photoionization efficiency curve of O_2^+ is due to autoionization from a small O_2 imputity. The Hopfield continuum was used at a resolution of 0.8 Å.

brational level in O_3^+ populated directly but not resolved in the PES experiments.

The location of the onset for the steps can be correlated well with the peaks observed in the first band of the photoelectron spectrum of ozone.[6] A summary of the results in the threshold region is shown in Table I. where our measurements are compared with those of Jonathan *et al.*,[6] Frost *et al.*,[7] and Brundle.[8] The results of Brundle were adjusted downward to bring the adiabatic ionization potential into better agreement with that of the other workers.

The irregular spacing between adjacent steps reported in this work seems to rule out any simple assignment[7,8] of the first photoelectron band to the ν_2 bending mode accompanying ionization from the $6a_1$, antibonding orbital. Jonathan and co-workers[6] explain the vibrational spacing by a Renner–Teller effect. Their assignment of a potential barrier however assumes that a very weak peak reported by them at 12.44 eV is the adiabatic I.P. Present results favor an adiabatic I.P. of 12.519 eV.

B. O_2^+

The ionization efficiency curve for the process $O_3 + h\nu \rightarrow O_2^+ + O + e$ is shown in Fig. 1. The sample of ozone partly decomposes to oxygen in the sample line and gives rise to the familiar autoionization structure[9] in the photoionization efficiency curve for O_2^+. Since the photoionization spectrum of oxygen near threshold is nearly all due to autoionization, the rise in the ionization efficiency curve for O_2^+ is entirely due to the formation of O_2^+ from O_3.

When corrected for internal thermal energy of 0.043 eV, this corresponds to a 0 °K threshold of 13.125 ± 0.004 eV, in good agreement with the accepted thermochemical threshold[10] of 13.120 eV based on the heats of formation of O_3 and O and the ionization potential of O_2. Hence, this measurement provides a satisfactory corroboration of the value for the heat of formation of O_3.

The second more intense rise in the O_2^+ photoionization efficiency curve occurs at 13.43$_2$ eV, and coincides with the adiabatic onset of the second excited state (third I.P.) of O_3^+ measured by photoelectron spectros-

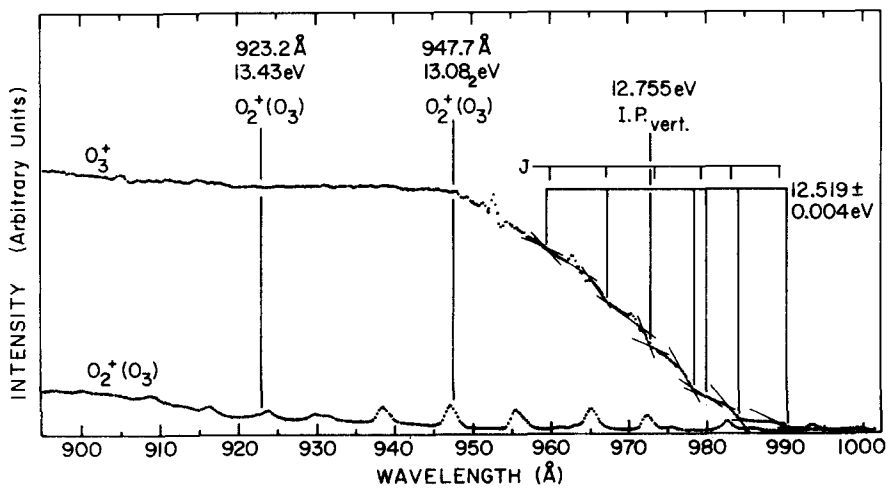

FIG. 2. Photoionization efficiency curves for O_3^+ and O_2^+ in the region near threshold. The lines are drawn to emphasize the steplike behavior of O_3^+ ionization near threshold. The onset of each step is compared with the photoelectron spectroscopic results of Jonathan and co-workers[6] (*J*). The peculiar structure in the wavelength region 950–972 Å is an experimental artifact due to the grating.

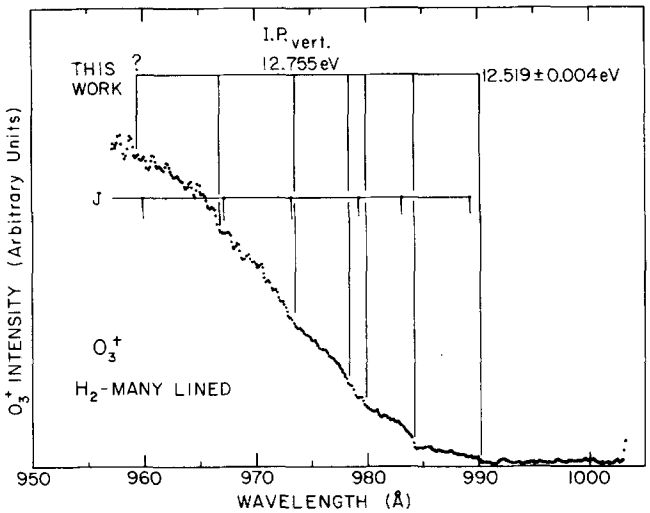

FIG. 3. Photoionization efficiency curve for O_3^+ near threshold using the hydrogen many-lined spectrum. Note the absence of the experimental artifacts observed in Fig. 2. The breaks in the curve closely correspond to the observed structure in the photoelectron work of Jonathan and co-workers.[6]

copy.[6-8] The photoelectron spectra of this band show it to be considerably broadened and it probably is largely predissociated.

Above the second onset of O_2^+ the intensity rises gradually, reaching a peak in the neighborhood of 730 Å (17.0 eV), afterwards steadily falling to 600 Å.

All of the structure in the O_2^+ photoionization efficiency curve can be identified with a O_2^+ contribution from a small O_2 impurity. The broad band in the 715–730 Å region is entirely due to O_2^+ from the oxygen impurity.

C. O^+

The ionization efficiency curve for the production of O^+ from ozone is structureless (Fig. 1). The initial departure of the O^+ signal from that of the linear background occurs at 15.21 ± 0.01 eV (Fig. 3), 0.57 eV above the thermochemical threshold for the process $O_3 + h\nu \rightarrow O_2\,(X^3\Sigma_g) + O^+\,(^3P)$.

A vertical I.P. of 15.57 eV from a weak photoelectron band has been reported by Jonathan and co-workers.[6] The observance of a weak onset of O^+ at 15.21 eV suggests it may be formed from the photoelectron band associated with the fourth I.P. of ozone.

The O^+ intensity continues to increase gradually from onset until 700 Å, where it ascends more steeply At 620 Å the O^+ signal begins to increase still more rapidly and continues to increase down to 600 Å, the usable limit of the Hopfield continuum.

The photoelectron spectra of ozone in the 14–20 eV region show a number of bands[6-8] that could be contributing to the O^+ signal by predissociating. The fourth and fifth electronic bands in O_3^+ are probably contributing to the weak O^+ signal down to 700 Å. The more intense increase below 700 Å can be ascribed to the participation of the sixth (vertical I.P.: 17.45 eV) and seventh (vertical I.P.: 19.99 eV) bands.

D. Fragmentation processes at 600 Å

The ratio of the parent to fragment ions in O_3 at 600 Å is O_3^+: O_2^+: O^+ = 1.00: 0.36: 0.05. Since the appearance of O_2 occurs at the thermochemical limit of 13.08_2 eV, the first electronic band of O_3^+ and most of the second band are not predissociated. At photon energies greater than 13.43 eV, the third band is largely predissociated to $O_2^+ + O$ and contributes to the rise in the O_2^+ signal. Appearance of O^+ ions at 15.21 eV and the continued rise in the O^+ signal can be plausibly ascribed to predissociation from the fourth, fifth, and sixth electronic states of O_3^+.

If the areas under the photoelectron bands are calculated, a correlation can be made between the relative abundances of the ions formed and the intensity of the particular bands probably responsible for the predissociation. Table II is a listing of the fragment: parent ratios observed in the studies together with the computed area under each of the photoelectron bands taken from the work of Jonathan *et al.*

If it is assumed that predissociation of O_3^+ occurs from "bound" molecular-ion states, the ratios of the fragment ion abundances in Table I should closely parallel the ratios of electronic band intensities observed in photoelectron spectroscopy. The results of this work show that the fragment ion abundances of O_2^+ and O^+ at 600 Å predicted on the basis of photoelectron band intensities are underestimated. There are two factors which can contribute to this effect.

With the exception of the thermochemical onset for

TABLE I. Photoionization of O_3—First Band.

Wavelength (Å)	Energy (eV)	Jonathan[a] *et al.*	Frost[b]	Brundle[c] −0.030
990.35	12.519 ± 0.004	12.53	12.53	12.53
983.75	12.603 ± 0.007	12.61	12.59	12.59
980.09	12.650 ± 0.008	...	...	...
977.78	12.689 ± 0.013	12.67	12.66	12.66
972.03	12.755 ± 0.014	12.75	12.74	12.74
966.27	12.831 ± 0.015	12.83	12.83	12.83
959.32	12.924 ± 0.007	12.92	12.90	12.90

[a]See Ref. 6.
[b]See Ref. 7.
[c]See Ref. 8.

TABLE II. Relative intensities of fragment ions in O_3 at 600 Å and intensitities of electronic bands in photoelectron spectroscopy.

Ion	Relative Intensity at 600 Å	Electronic Band	Photoelectron[a] Band Intensity
O_3^+	1.00	I, II	1.00
O_2^+	0.36	III[b]	0.52
O^+	0.05	IV–VII	0.28

[a]Reference 6
[b]Some contribution of the upper levels of the second band are included in the intensity of the third band.

O_2^+ at 947.7 Å, fragment ions are produced with variable but unknown amounts of kinetic energy. Previous experimental results with the apparatus[11] show that ions formed with kinetic energies $\gtrsim 0.5$ eV are not collected with high efficiency. The energy discrimination would more adversely affect the collection of O^+ ions than O_2^+ and this seems to be borne out in Table II.

The other factor which could affect the discrepancy between the mass spectrometric and photoelectron results would be the enhanced collection efficiency of a photoelectron apparatus for low kinetic energy photoelectrons. The higher electronic states of O_3^+ are presumed to predissociate to O^+ (Table II). Two of these bands are very intense and lie in a region where the photoelectrons have a kinetic energy $\gtrsim 1$ eV. Any explanation for the disparity between the two types of measurements would have to consider in addition to the ion kinteic energy discrimination of the mass analyzer, the problem of electron kinetic energy discrimination of these two photoelectron bands and to a lesser extent, bands in the 16–18.5 eV region of the photoelectron spectrum.

Further answers to the problem of ion kinetic energy discrimination in ozone must await measurements on mass analyzers of the type reported by Fryar and Browning,[12] which attempt to minimize ion discrimination due to kinetic energy.

E. O_5^+

O_5^+ ion formation was detected in the ozone experiments. The ozone pressure was adjusted until the O_5^+ intensity was 5% that of O_3^+. Under these conditions, the ozone pressure in the ionization chamber was estimated to be 1×10^{-4} Torr. The O_5^+ signal was found to vary quadratically with the ozone pressure, hence the probable mechanism of formation would be via the ion–molecule reaction

$$O_3^+ + O_3 \rightarrow O_5^+ + O \,. \qquad (1)$$

The photoionization efficiency curve for O_5^+ as a function of wavelength is shown in Fig. 4. Onset for O_5^+

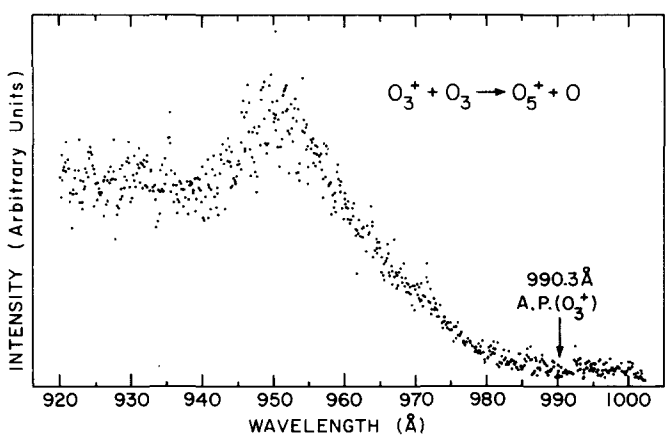

FIG. 4. Photoionization efficiency curve for O_5^+ using the Hopfield continuum. The sharp decline in intensity beginning at 950 Å may be due to the dissociation channel $O_5^+ \rightarrow O_2^+ + O_3$ (see text).

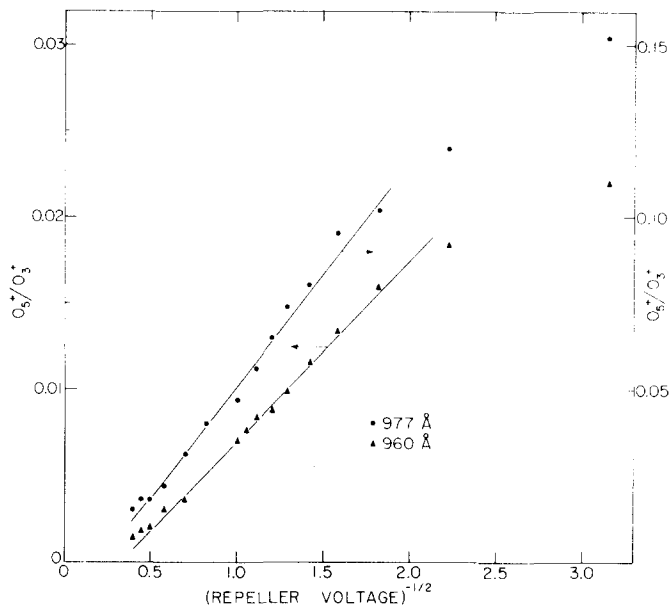

FIG. 5. The dependence of the ratio O_5^+/O_3^+ on the repeller field strength, V_{rep}, for the reaction $O_3^+ + O_3 \rightarrow O_5^+ + O$. Upper curve: $\lambda = 977$ Å. Lower curve: $\lambda = 960$ Å.

production appears, within limits of detection, to be identical to that of O_3^+, indicating that the above reaction is thermoneutral or exothermic.

An interesting feature of the O_5^+ curve is the rapid falloff of O_5^+ intensity with wavelength in the region 950–940 Å. One explanation for this behavior is that O_5^+ formed in this wavelength region acquires sufficient internal energy to dissociate. The heat of formation of O_5^+ is 12.99 eV, assuming the reaction $O_3^+ + O_3 \rightarrow O_5^+ + O$ is thermoneutral. The likely mode of decay of O_5^+ is the process $O_5^+ \rightarrow O_2^+ + O_3$, which would be endothermic by 0.58 eV. If this endothermicity is added to the appearance potential and O_3^+, one arrives at 13.10 eV or 946 Å for the onset of O_2^+, about the same wavelength at which the O_5^+ begins to fall off.

Since the Langevin cross section should be inversely proportional to velocity, the behavior of the ion–molecule Reaction (1) was studied as a function of the inverse square root of the repeller voltage at two different wavelengths. These results are plotted as shown in Fig. 5. At nearly all but the lowest repeller voltages the curves showed linear behavior with no apparent dependence on the wavelength. A separate study also showed no significant dependence of the O_5^+/O_3^+ ratio on wavelength.

An estimation of the cross section for O_5^+ formation can be made assuming a pressure of 1×10^{-4} Torr in the ionization region, a path length of 1 cm and a O_5^+/O_3^+ ratio of 0.05. The cross section can be calculated from the simple relation $\sigma = (I_{O_5^+}/I_{O_3^+})/Npl$, where N is the concentration of molecules per Torr, l is the path length, and p is the ozone pressure, in Torr. The cross section under these conditions is calculated to be 143 Å^2. This is to be compared with the theoretical Langevin cross section $\sigma_{theor\,1/2}$, given by the expression[13] $\sigma_{theor} = (2\pi e/v_0)(\alpha/\mu)^{1/2}$. Here e is the electronic

charge, v_0 is the ion velocity, α is the polarizability of the target, and μ is the reduced mass. Using an estimated polarizability of 4×10^{-24} cm^2, the Langevin cross section for 1 eV O_3^+ ions in the laboratory system is 40 Å^2, which compares favorably with the experimental estimate of 143 Å^2 and shows that reaction probably occurs on every collision.

F. O_4^+

The O_4^+ ion was also detected at a maximum intensity of about 2% relative to that of O_5^+. The O_4^+ signal intensity was found to be linear with O_3 and O_2 pressure, respectively, and would seem to rule out O_4^+ formation via the process $O_3+O_3^+\rightarrow O_4^++O_2$. Taking the heat of formation ΔH_f^0 for O_4^+ to be 11.60 eV, based on the experimental determination of $D_0(O_2-O_2^+)$ of 0.46 eV by Conway and Janik,[14] the exothermicity for the latter process is 3.96 eV, which is probably too high for the reaction intermediate to survive.

Two possible mechanisms for O_4^+ formation would be by the reactions

$$O_2^++O_3\rightarrow O_4^++O \tag{2}$$

and

$$O_2+O_3^+\rightarrow O_4^++O, \tag{3}$$

which are endothermic by 2.09 eV and 0.12 eV, respectively. Reaction (2) can be ruled out as O_4^+ is observed near the threshold for O_3^+ formation. This leaves (3) as the probable source of O_4^+ ions. Since the O_4^+ intensity was observed to be quite small relative to O_5^+ when the O_2 and O_3 concentrations were approximately equal, Reaction (1) must compete very effectively with (3).

*Work performed under the auspices of the Energy Research and Development Administration.

†On Sabbatical leave from the Hebrew University of Jerusalem, Department of Physical Chemistry, Jerusalem, Israel 91000.

[1]For a complete listing, see R. D. Hudson, Can. J. Chem. 52, 1465 (1974).
[2]Y. Tanaka, E. C. Y. Inn, and K. Watanabe, J. Chem. Phys. 21. 1651 (1953).
[3]M. Ogawa and G. R. Cook, J. Chem. Phys. 28, 173 (1958).
[4]G. R. Cook, in *Recent Developments in Mass Spectroscopy*, edited by K. Ogata and T. Hayakawa (University Park, Baltimore, 1970), 761.
[5]J. Berkowitz and W. A. Chupka, J. Chem. Phys. 45, 1287 (1966); W. A. Chupka and J. Berkowitz, J. Chem. Phys. 47, 2921 (1967).
[6]J. M. Dyke, L. Golob, N. Jonathan, A. Morris, and M. Okuda, J. Chem. Soc. Faraday Trans. 2, 1828 (1974).
[7]D. C. Frost, S. T. Lee, and C. A. McDowell, Chem. Phys. Lett. 24, 149 (1974).
[8]C. R. Brundle, Chem. Phys. Lett. 26, 25 (1974).
[9]B. Brehm, Z. Naturforsch. Teil A 21, 196 (1966); F. M. Matsunaga and K. Watanabe, Sci. Light Tokyo 16, 31 (1967); V. H. Dibeler and J. A. Walker, J. Opt. Soc. Am. 57, 1007 (1967); P. M. Dehmer and W. A. Chupka, J. Chem. Phys. 62, 4525 (1975).
[10]JANAF Thermochemical Tables (Dow Chemical Co., Midland, MI, 1963).
[11]Paula L. Kronebush and J. Berkowitz, "Photodissociative ionization in the 21–41 eV region: O_2, N_2, CO, NO, CO_2, H_2O, NH_3, and CH_4" Int. J. Mass. Spectrom. Ion Phys. 22. 283 (1976).
[12]J. Fryar and R. Browning, Planet. Space Sci. 21, 709 (1973).
[13]E. W. McDaniel, *Collision Phenomena in Ionized Gases* (Wiley, New York, 1964), Secs. 3.6 and 6.3, Appendix II.
[14]D. C. Conway and G. S. Janik, J. Chem. Phys. 53, 1859 (1970).